Chemical Physics Letters 456 (2008) 27–30

Contents lists available at ScienceDirect

Chemical Physics Letters

journal homepage: www.elsevier.com/locate/cplett

Formation of hydrogen peroxide and water from the reaction of cold hydrogen atoms with solid oxygen at 10 K

N. Miyauchi *, H. Hidaka, T. Chigai, A. Nagaoka, N. Watanabe, A. Kouchi

Institute of Low Temperature Science, Hokkaido University, N19-W8, Kita-ku, Sapporo 060-0819, Japan

ARTICLE INFO

Article history:
Received 11 January 2008
In final form 26 February 2008
Available online 2 March 2008

ABSTRACT

The reactions of cold H atoms with solid O_2 molecules were investigated at 10 K. The formation of H_2O_2 and H_2O has been confirmed by *in situ* infrared spectroscopy. We found that the reaction proceeds very efficiently and obtained the effective reaction rates. This is the first clear experimental evidence of the formation of water molecules under conditions mimicking those found in cold interstellar molecular clouds. Based on the experimental results, we discuss the reaction mechanism and astrophysical implications.

1. Introduction

Water is the most abundant solid material in space, and has been observed in various astrophysical environments, such as outer planets, satellites, comets, and interstellar clouds [1]. Since the solar system evolved from an interstellar molecular cloud, icy objects in the solar system originated from the water ice formed in the interstellar molecular cloud. Therefore, gaining an understanding of the origin of water molecules in interstellar molecular clouds is critical not only for discussing the origin of the solar system, but also for understanding chemical evolution and the origin of life [2]. However, the formation mechanism of water molecules in the interstellar clouds has not been understood to date. It has been clarified that the formation of water molecules in the gas phase is incapable of explaining the observed abundance in molecular clouds [3,4]. Thus, it has been suggested that water molecules are synthesized by atomic reactions involving H and O on pre-existing silicate or carbonaceous grains at around 10 K [3–5].

The first possible process for H_2O formation is the sequential hydrogenation of O atoms on grains

$$O + H \rightarrow OH, \qquad (1)$$
$$OH + H \rightarrow H_2O. \qquad (2)$$

These reactions have no activation barriers [6]. The second possible process is the reaction of OH with hydrogen molecules absorbed on the surface of grains

$$OH + H_2 \rightarrow H_2O + H, \qquad (3)$$

which has an activation energy of 5.16 kcal/mol in the gas phase [7]. For the third process, Tielens and Hagen [8] proposed alternative reactions

$$O + O \rightarrow O_2, \qquad (4)$$
$$O_2 + H \rightarrow HO_2, \qquad (5)$$
$$HO_2 + H \rightarrow H_2O_2, \qquad (6)$$
$$H_2O_2 + H \rightarrow H_2O + OH. \qquad (7)$$

Reaction (5) has essentially no barrier; theoretically estimated activation energies lie between 0.1 and 0.4 kcal/mol [9]. Reaction (7) has activation energies of 3.6–4.3 kcal/mol [10]. All activation energies referred here are value in the gas phase. There has been no data available on a surface. Fig. 1 summarizes the possible water formation routes from reactions (1)–(7). Cuppen and Herbst [6] simulated the formation of water molecules in various environments of interstellar clouds, and found that reactions (1) and (2) are the main routes in cool diffuse clouds and reactions from (3)–(7) are the main routes in cold molecular clouds. H and O atoms are the major gas-phase species in the former clouds, whereas H_2 molecules are the major gas-phase species in the latter clouds.

Hiraoka et al. [11] investigated reactions (1) and (2) by spraying D atoms onto O atoms trapped in an N_2O matrix at 12 K. They analyzed the products by using temperature-programmed desorption (TPD) spectroscopy and observed D_2O. A similar experiment has been performed by Dulieu et al. [12] although their results are still very preliminary. However, in the experiments of both groups, it remains unclear whether D_2O is formed at 10–12 K or during heating. It is essential to perform *in situ* analysis during H/D atom irradiation to confirm the formation temperature of H_2O and to obtain kinetic data. For reactions (5)–(7), Klein and Scheer [13] performed pioneering experiments on the reaction of H atoms with solid O_2 at

---

* Corresponding author. Fax: +81 11 706 7142.
E-mail address: naoya@lowtem.hokudai.ac.jp (N. Miyauchi).

0009-2614/$ - see front matter © 2008 Elsevier B.V. All rights reserved.
doi:10.1016/j.cplett.2008.02.095

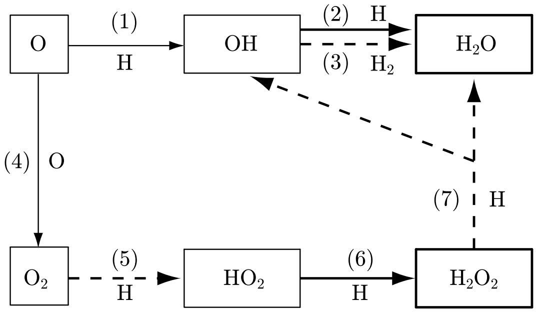

Fig. 1. Possible reaction scheme for formation of H_2O involving H and O atoms in interstellar clouds (modified from [5,8]). Atoms or molecules and numerals next to the arrows indicate the reactants in the reaction and the number of the reaction in the text, respectively. Broken and solid arrows indicate reactions with and without activation barriers, respectively. Thick and thin arrows denote reactions investigated and not investigated in the present study, respectively. Molecules observed in the present study are enclosed in thick squares.

20 K. Although they speculated on the production of H_2O_2 and H_2O based on their experimental results, they were unable to verify the production of these molecules since no analysis of the products was performed. To investigate the formation mechanism of water molecules in interstellar molecular clouds, we focus on reactions (5)–(7) and the subsequent reactions (2) and (3), and performed H/D addition experiments to solid O_2 at 10 K.

2. Experimental

Experiments were performed using the Apparatus for SUrface Reaction in Astrophysics (ASURA) system described previously [14,15]. Briefly, solid O_2 with an 8 monolayer (ML) thickness was produced by vapor deposition on an aluminum substrate at 10 K at a deposition rate of 25 pm s^{-1} in an ultrahigh vacuum chamber at a pressure of about 10^{-8} Pa. Atomic H and D were produced by a microwave-induced plasma in a Pyrex tube and transferred via a series of PTFE and aluminum tubes to the target. The dissociation fraction was about 20% at least. The atomic beams could be cooled to 20 K in the aluminum tube that was connected to an He refrigerator. The flux of atoms was controlled by varying the temperature of the aluminum tube and measured by the method of Hidaka et al. [16]. The fluxes of both the H and D atoms were 2×10^{14} cm^{-2} s^{-1} in the present experiments. Infrared absorption spectra of the sample solid during irradiation by atoms were measured *in situ* by Fourier transform infrared spectroscopy with a resolution of 4 cm^{-1}. After irradiation, TPD spectra of the sample were obtained using a quadrupole mass spectrometer at a heating rate of 4 K min^{-1}.

3. Results and discussion

Fig. 2a shows the change in a typical absorption spectra on irradiation by 70 K-hydrogen atoms at 10 K. This figure shows the absorbance variations from the initial spectrum of the sample, so that bands appearing above the baseline indicate an increase in absorbance. H_2O_2 appears immediately with bands at 3250, 2830, and 1405 cm^{-1}, then H_2O follows at 3432, 1650, and 820 cm^{-1}. No product was observed when solid O_2 was exposed to an H_2 beam at 10 K, or when H atoms were sprayed onto the Al substrate without solid O_2, demonstrating that the formation of H_2O_2 and H_2O in the present experiments is due to H atom irradiation onto O_2. No intermediate radicals (e.g., HO_2) were observed, suggesting that the reaction rate of (5) is much slower than that of (6). In this experiment, the H flux is sufficiently large so that the reaction (5) immediately proceeds to produce HO_2. The formation of H_2O_2 and H_2O were also observed when solid O_2 was exposed to an H beam at temperatures between 15 K and 20 K. Fig. 2b clearly reveals the production of D_2O_2 and D_2O in D-exposure experiments, confirming that the H_2O produced in the present experiments is not a contaminant. The production of $H_2O_2(D_2O_2)$ and $H_2O(D_2O)$ was also indicated in TPD spectra obtained after H(D)-exposure.

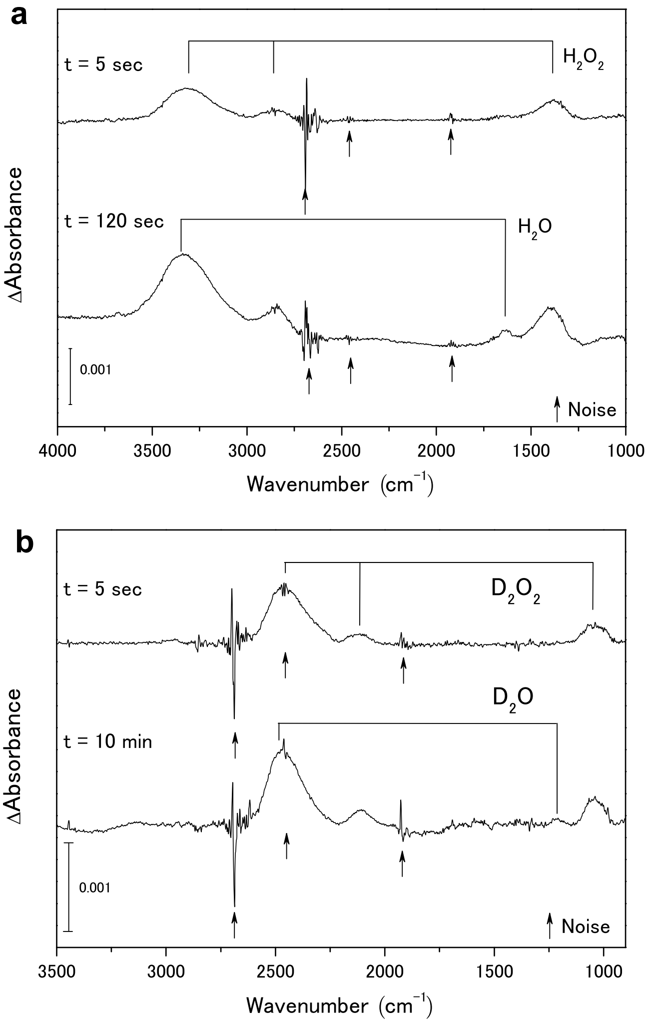

Fig. 2. Spectral change in solid O_2 due to (a) cold H exposure and (b) D exposure. The spectra were obtained by subtracting the initial absorption spectra of non-irradiated samples from the spectra of H(D)-irradiated samples. Lines indicate newly formed molecules. Spikes with arrows indicate noise caused by vibration of the He refrigerator.

The amount of products are calculated and plotted as a function of exposure time in Fig. 3. These were obtained from the band areas in the spectra and the reported and estimated integrated band strengths. The integrated band strengths used are 1.2×10^{-17} and 2.1×10^{-17} molecule cm^{-1} for H_2O (1655 cm^{-1}) [17] and H_2O_2 (1347 cm^{-1}) [18], respectively. Since no integrated band strengths for D_2O at 1200 cm^{-1} and D_2O_2 at 1033 cm^{-1} have been reported, we estimated these in the following manner. Bergren et al. [19] measured the optical constants of OH(OD)-stretching modes in amorphous H_2O and D_2O at 3200 cm^{-1} and 2400 cm^{-1}, respectively. Assuming that the ratio of integrated band strengths for H_2O and D_2O in OH(OD)-stretching modes are the same as those in OH(OD)-bending modes, we estimated the integrated band strength of OD-bending modes for D_2O (1200 cm^{-1}) to be 8×10^{-18} molecule cm^{-1}. No data is available for D_2O_2, not even optical constants. So we assumed that the ratio of integrated band strengths for $H_2O/D_2O = 0.67$ is the same as that for H_2O_2/D_2O_2, and estimated the integrated band strength of OD-bending modes for D_2O_2 (1033 cm^{-1}) to be 1.5×10^{-17} molecule

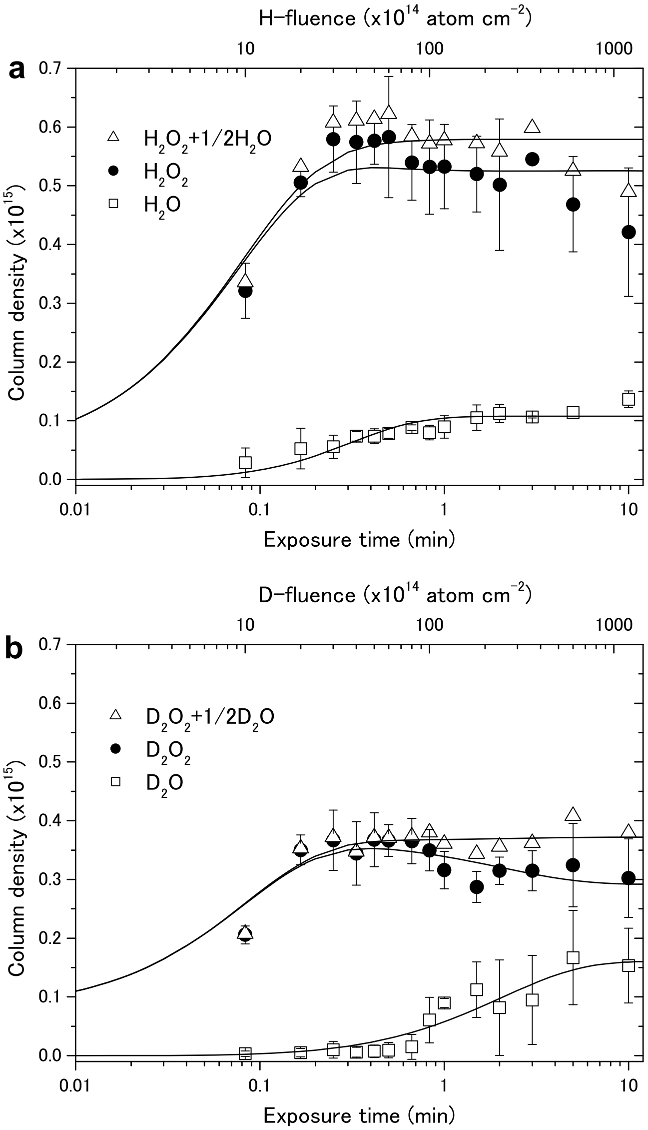

Fig. 3. Variation in column densities of products (a) for H_2O_2 and H_2O with H exposure and (b) for D_2O_2 and D_2O with D exposure. Each data point represents the average of three measurements, and error bars represent the statistical errors. The upper abscissa indicates the fluence of H(D) atoms. The solid lines are fitted to the curves defined by Eqs. (12)–(14). The amount of O_2 reduction is assumed to be equal to the sum of the increase in H_2O_2 (D_2O_2) and 1/2H_2O (1/2D_2O). Fitting curves of H_2O and D_2O shown are two times larger than those obtained from Eq. (14).

cm^{-1}. This result is consistent with the spectral features of OH and OD-bending modes of amorphous H_2O_2 and D_2O_2 measured by Lannon et al. [20], which show that the ratio of peak heights for H_2O_2/D_2O_2 is 0.75.

Fig. 3a clearly shows that the formation of H_2O_2 and H_2O is very rapid and efficient; H_2O_2 and H_2O are observed even after exposure for 5 s. When H atoms are irradiated onto solid CO at 10 K [14], the production of H_2CO and CH_3OH are observed after 30 s and 1 min, respectively. The present experimental results confirm that reactions (5)–(7), which were initially proposed based on theoretical considerations [8,6], proceed at 10 K. Since reaction (5) essentially has no barrier [9], it is natural that this reaction proceeds very rapidly. While reaction (7) has an activation energy of 3.6–4.3 kcal/mol [10], it has been suggested that this reaction does not proceed by an Arrhenius-type reaction at 10 K, but rather proceeds by a tunneling reaction even at 10 K. As described later, isotope effect (H or D) on reaction (7) has been observed, strongly supporting that reaction (7) proceeds by the tunneling reaction. After the formation of OH by reaction (7), there are two possible reaction routes for further H_2O formation: reactions (2) and (3). This is because the H-beams used in the present experiments do not consist of pure H atoms, but rather are a mixture of H and H_2. Reaction (2) has no activation barrier, while the activation energy of reaction (3) is 5.16 kcal/mol [7]. It seems probable that H_2O is formed by reaction (2), although we currently have no direct evidence for this. Fig. 3b shows that D_2O_2 and D_2O are produced very rapidly and efficiently in the D-exposure experiments, although the formation of D_2O is slightly slower than in H-exposure experiments.

In the present experiments, it is impossible to directly measure the decrease in O_2, since O_2 is infrared inactive. Thus, it is reasonable to assume that the summation of 0.5H_2O and H_2O_2 is equal to the reduction of O_2. The O_2 loss becomes saturated after long exposure. This type of saturation was also found previously for the successive hydrogenation of CO at 8–15 K by Watanabe et al. [14,21]. They concluded from the dependence of the saturation value on the sample thickness that the saturation is related not to the balance between the forward and reverse reactions, but rather to the diffusion length of H in solid CO and CO–H_2O mixed ice. This suggests that in the present experiments the reaction occurs only at the surface. The structure of the molecular layer may thus be onion-like, with H_2O on the top, H_2O_2 in the middle, and O_2 at the bottom. The amount of H_2O_2 is greater than that of D_2O_2, suggesting that the diffusion length of H into O_2 is longer than that of D into O_2. On the other hand, the amount of H_2O is the same as that of D_2O, suggesting that the water formation reaction occurs only at surface. The small amount of observed H_2O compared to H_2O_2 may be attributed to desorption of products caused by the release of the heat of reaction.

To discuss the reaction mechanism based on the isotope effect, we next derive effective reaction rate constants by fitting the data in Fig. 3. To simplify the problem, we assume that reactions (5)–(7), (2) and (3) can be simplified to the following consecutive reaction:

$$O_2 \xrightarrow{k_1} H_2O_2 \xrightarrow{k_2} 2H_2O, \tag{8}$$

where k_i is the reaction rate constant of the ith reaction. Since, it is very difficult to measure the surface density of H atoms, n_H, in the present study, we were not able to obtain k_i directly. Instead, we define effective rate constants: $k'_{Hi} = k_i n_H$. Since n_H is considered to be time-independent, these reactions are assumed to be pseudo-first-order reactions.

Furthermore, we assume that the products have a layered structure, as mentioned above. In the deepest layer, no reaction of O_2 with H atoms occurs. In the middle layer that has a thickness of a, the reaction from O_2 to H_2O_2 occurs, but that from H_2O_2 to H_2O does not occur. In the uppermost layer with a thickness of b, the entire reaction (8) occurs. The rate equations for the number densities n_i of O_2, H_2O_2 and H_2O are given by

$$\frac{dn_0}{dt} = -k'_{H1} n_0, \tag{9}$$

$$\frac{dn_1}{dt} = k'_{H1} n_0 - k'_{H2} n_1, \tag{10}$$

$$\frac{dn_2}{dt} = 2k'_{H2} n_1. \tag{11}$$

The solutions of Eqs. (9)–(11) for the initial conditions of $n_0(t = 0) = n_0^0$, and $n_1(0) = n_2(0) = 0$ are given by

$$\frac{n_0}{n_0^0} = b e^{-k'_{H1}t} + a e^{-k'_{H1}t}, \tag{12}$$

$$\frac{n_1}{n_0^0} = b \frac{k'_{H1}}{k'_{H1} - k'_{H2}} \left(e^{-k'_{H2}t} - e^{-k'_{H1}t} \right) + a \left(1 - e^{-k'_{H1}t} \right), \tag{13}$$

$$\frac{n_2/2}{n_0^0} = b \left[1 + \frac{1}{k'_{H1} - k'_{H2}} \left(k'_{H2} e^{-k'_{H1}t} - k'_{H1} e^{-k'_{H2}t} \right) \right], \tag{14}$$

Table 1
Effective reaction rate constants (min^{-1})

Temperature (K)	Reaction					
	O_2 + H k'_{H1}	H_2O_2 + H k'_{H2}	O_2 + D k'_{D1}	D_2O_2 + D k'_{D2}	CO + H k'_{H3}	CO + D k'_{D3}
10	12.8	3.9	12.0	0.49	0.14[a]	0.014[b]
15					0.41[c]	0.033[c]

a, b, c: obtained with the H(D) flux of 1×10^{14} cm^{-2} s^{-1} [22].
[a] For pure CO [15].
[b] For pure CO [16].
[c] For 0.8 ML CO on amorphous H_2O [16].

where $n_0 + n_1 + n_2/2 = n_0^0$. In the case of D exposure, the same reaction as that for H exposure is assumed to occur, namely,

$$O_2 \xrightarrow{k'_{D1}} D_2O_2 \xrightarrow{k'_{D2}} D_2O, \tag{15}$$

where $k'_{Di} = k_i n_D$, and n_D is the surface density of D atoms. Effective rate constants, k'_{Hi} and k'_{Di}, obtained by fitting the data are shown in Table 1 together with those for the first steps of successive hydrogenation (deuteration) of CO [15,16]:

$$CO \xrightarrow{k'_{H3}} HCO \rightarrow H_2CO \rightarrow CH_3O \rightarrow CH_3OH, \tag{16}$$

$$CO \xrightarrow{k'_{D3}} DCO \rightarrow D_2CO \rightarrow DH_3O \rightarrow DH_3OD. \tag{17}$$

Using the relation of $n_H/n_D = 1$ [16], the ratios of the reaction rate constants are estimated: $k'_{H1}/k'_{D1} = 1$ and $k'_{H2}/k'_{D2} = 8$. The former result states that there is no difference in rate constants between O_2 + H and O_2 + D at 10 K, and it is consistent with the fact that reaction (5) has essentially no barrier [9]. The latter result for the ratio of reaction rate constants between H_2O_2 + H and D_2O_2 + D ($k'_{H2}/k'_{D2} = 8$) is reasonable for a tunneling reaction with an activation energy of 3.6–4.3 kcal/mol [10]. In the case of CO + H(D), the ratio of reaction rate constants, k'_{H3}/k'_{D3}, lies between 10 (from Table 1) and 13 [16] with an activation energy of about 4 kcal/mol. In any case, these data are very useful for estimating the barrier height and width of a potential, and potential energy surface as discussed by Hidaka et al. [16]. As already mentioned qualitatively, the rate constants of (8) and (15) are one to two orders of magnitude greater than those of (16) and (17).

4. Astrophysical implications

Our results have several implications for ice in space. Assuming a hydrogen number density of 1 cm^{-3}, the H fluences in a 10 K molecular cloud will be 1.3×10^{16} and 1.3×10^{17} cm^{-2} over 10^4 and 10^5 years, respectively. In the present experiment, these fluences approximately correspond to exposure times of 1 and 10 min. Considering that the lifetime of molecular clouds is of the order of 10^6 years, it is reasonable to say that water formation by reactions (5)–(7) occurs very quickly in molecular clouds. Based on computer simulations of surface reaction networks, Tielens and Hagen [8] and Cuppen and Herbst [6] conjectured that reactions (4)–(7) occur in cold molecular clouds in which the ratio H/H_2 is low. The present results strongly support their conclusion experimentally, although the contribution of reactions (1)–(3) is still unclear.

Solid O_2 is expected to occur on the grain surface with H_2O and CO ice in interstellar molecular clouds and to be observable by infrared telescopes since the 6.44 μm O=O stretching mode is observable when O_2 is surrounded by other molecules [23] and because the 4.67 μm feature of CO is altered when O_2 is mixed with CO [24]. However, no positive detection has been reported so far [24]. Present experiments clearly explain why no O_2 has been observed: if an O_2 molecule is formed on grain surface it will react very quickly with H to form H_2O_2 and H_2O within 10^{4-5} years as shown in Fig. 3a.

Recent astronomical observations have revealed that the abundances of some deuterated molecules are up to four orders of magnitude greater than the cosmic D/H ratio of 1.5×10^{-5}. In the case of water, a HDO/H_2O ratio of 0.03 has been measured in a solar-type protostar [25]. Many theoretical models, including pure gas phase models [26] and gas-grain models [27], have been proposed. However, only a few experimental studies have been performed to verify the latter models [16,28]. In the case of formaldehyde and methanol, the successive addition of D to CO (reaction (17)) is not favorable for producing deuterated formaldehyde and methanol [16]. Instead, H–D substitution in formaldehyde and methanol are necessary to achieve the observed abundances of deuterated spiecies [28]. However, Nagaoka et al. [28] found experimentally that no deuteration of H_2O occurs by H–D substitution under D exposure at 10–20 K, even for fluences of up to 5×10^{18} cm^{-2}. Considering the ratios of $k'_{H1}/k'_{D1} = 1$ and $k'_{H2}/k'_{D2} = 8$ obtained in the present experiments and the D/H atom ratio of 0.1 or less expected in molecular clouds [29], deuterium addition to O_2 is favorable for producing the observed amount of HDO; the observed HDO/H_2O ratio of 0.03 can be achieved in a time scale between 10^4 and 10^5 years. Although the discussion is indefinite at present, the experimental results presented in this study provide a basis for discussing H/D fractionation.

Acknowledgements

This work was partly supported by a Grant-in-Aid for Scientific Research from the Japan Society for the Promotion of Science and the Ministry of Education, Science, Sports, and Culture of Japan.

References

[1] B. Schmitt, C. de Bergh, M. Festou (Eds.), Solar System Ices, Kluwer, Dordrecht, 1998.
[2] J. Chela-Flores, F. Raulin (Eds.), Chemical Evolution: Physics of the Origin and Evolution of Life, Kluwer, Dordrecht, 1996.
[3] L.B. d'Hendecourt, L.J. Allamandola, J.M. Greenberg, Astron. Astrophys. 152 (1985) 130.
[4] T.I. Hasegawa, E. Herbst, C.M. Leung, Astrophys. J. Suppl. 82 (1992) 167.
[5] A.G.G.M. Tielens, The Physics and Chemistry of the Interstellar Medium, Cambridge University Press, Cambridge, 2005.
[6] H.M. Cuppen, E. Herbst, Astrophys. J. 668 (2007) 294.
[7] H.I. Schiff, in: B.M. McCormac (Ed.), Physics and Chemistry of Upper Atmospheres, Reidel, Dordrecht, 1973, p. 85.
[8] A.G.G.M. Tielens, W. Hagen, Astron. Astrophys. 114 (1982) 245.
[9] S.P. Walch, C.M. Rohlfing, C.F. Melius, C.W. Bauschlicher Jr., J. Chem. Phys. 88 (1988) 6273.
[10] H. Koussa, M. Bahri, N. Jaidane, Z. Ben Lakhdar, J. Mol. Struct.—Theochem 770 (2006) 149.
[11] K. Hiraoka et al., Astrophys. J. 498 (1998) 710.
[12] F. Dulieu et al., in: S. Diana, J.L. Lemaire, (Eds.), Abstracts of Molecules in Space & Laboratory, Paris, 2007, p. 124.
[13] R. Klein, M.D. Scheer, J. Chem. Phys. 31 (1959) 278.
[14] N. Watanabe, A. Nagaoka, T. Shiraki, A. Kouchi, Astrophys. J. 616 (2004) 638.
[15] N. Watanabe et al., Planet. Space Sci. 54 (2006) 1107.
[16] H. Hidaka, A. Kouchi, N. Watanabe, J. Chem. Phys. 126 (2007) 204707.
[17] P.A. Gerakins, W.A. Schutte, J.M. Greenberg, E.F. van Dishoeck, Astron. Astrophys. 296 (1995) 810.
[18] M.L. Loeffler, B.D. Teolis, R.A. Baragiola, J. Chem. Phys. 124 (2006) 104702.
[19] M.S. Bergren, D. Schuh, M.G. Sceats, S.A. Rice, J. Chem. Phys. 69 (1978) 3477.
[20] J.A. Lannon, F.D. Verderame, R.W. Anderson Jr., J. Chem. Phys. 54 (1971) 2212.
[21] N. Watanabe, T. Shiraki, A. Kouchi, Astrophys. J. 588 (2003) L121.
[22] N. Watanabe et al., Astrophys. J. 668 (2001) 1001.
[23] P. Ehrenfreund, R. Breukers, L. dfHendecourt, J.M. Greenberg, Astron. Astrophys. 260 (1992) 431.
[24] B. Vandenbussche et al., Astron. Astrophys. 346 (1999) L57.
[25] B. Parise et al., Astron. Astrophys. 431 (2005) 547.
[26] H. Roberts, T.J. Miller, Astron. Astrophys. 361 (2000) 388.
[27] A.G.G.M. Tielens, Astron. Astrophys. 119 (1983) 177.
[28] A. Nagaoka, N. Watanabe, A. Kouchi, Astrophys. J. 29 (2005) L29.
[29] H. Roberts, E. Herbst, T.J. Miller, Mon. Not. R. Astron. Soc. 340 (2002) 283.